Guiding properties of a non-isothermal atmosphere for acoustic-gravity waves

L. CANELLA [1], B. COSTANTINI [1], G. NALESSO [1] and A. R. JACOBSON [2]

[1] *INFM, Dipartimento di Elettronica e Informatica, Università di Padova*
Via Gradenigo 6/A, 35131 Padova, Italy
[2] *Space and Atmospheric Sciences Group - Mail Stop D466*
Los Alamos National Laboratory - Los Alamos, NM 87545, USA

(ricevuto il 20 Maggio 1996; revisionato il 15 Maggio 1997; approvato il 5 Giugno 1997)

Summary. — The propagation of pressure waves in a stratified, non-isothermal atmosphere is studied in the linear approximation. It is found that acoustic and acoustic-gravity waves can be horizontally guided by the effect of the Earth's thermocline alone, under very mild conditions on the temperature gradient steepness. The effect of the Earth's surface is also studied. Lamb's modes associated with the rigid surface are, then, identified and their behaviour, as a function of the Earth's position, is discussed. Finally, dissipation is included, and its effect is derived using a perturbation technique.

PACS 94.10.Jd – Tides, waves, and winds.

1. – Introduction

The capability of the terrestrial atmosphere to guide pressure waves has been known for a long time (Lamb, 1924; Pekeris, 1948). However, due to the complexity of the dependence on height of the equilibrium quantities, the characteristics of the guided modes (dispersion relation, localization, phase and group velocity) as well as the main physical driving mechanisms are difficult to identify.

Perhaps the most extensive analysis of guided modes in a realistic atmospheric model has been presented by Francis (1973, 1975). His results, although numerical, are very general and cover the entire spectrum of waves. He includes also practically all the physical effects, like dissipation, presence of the Earth's surface, realistic variation with height of the temperature, etc.

However, the completeness of Francis' model is also, in a sense, a weakness. It is often impossible, and usually at least not straightforward, to discriminate between the different effects and to assess the relative relevance of the various factors in driving the waves.

A further weakness, common however to all numerical analyses, is the difficulty of performing a parameter study.

Recently, by considering a simplified non-isothermal model, which nonetheless goes a step further of the classic model of a stratified isothermal atmosphere (see, *e.g.*, Yeh and Liu, 1974), we have been able to show the existence of acoustic and acoustic-gravity waves guided only by the temperature gradient (Nalesso and Jacobson, 1993). In the model we assumed a specific analytic, monotonically increasing with height, temperature profile. In this paper we will prove, more generally, the existence of horizontally guided modes for a large class of monotonic temperature profiles, and will find sufficient conditions for the existence of such waves.

We will, then, study, the behavior of the physical quantities such as pressure, density and fluid velocity components, as a function of the parameters which characterize the analytic profile considered in the previous article (Nalesso and Jacobson, 1993), and will show that the spectrum of ducted waves is indeed extraordinarily rich.

Furthermore, we will analyze the effect of including the Earth surface in the previous model and will show that Lamb's modes (Lamb, 1924; Francis, 1973) appear and how they evolve as the position of the rigid boundary is varied.

Finally, we will treat, using a perturbation approach, the effect of dissipation (viscosity and thermal conductivity) on the propagation of the eigenmodes.

2. – The stratified non-isothermal atmospheric model

The linearized hydrodynamics (HD) equations for a stratified, inviscid, infinite fluid, without source terms read

$$\partial\varrho/\partial t + \varrho_0 \nabla\cdot\mathbf{v} + \mathbf{v}\cdot\nabla\varrho_0 = 0 \,, \tag{1a}$$

$$\varrho_0 \partial\mathbf{v}/\partial t + \nabla p - \varrho\mathbf{g} = 0 \,, \tag{1b}$$

$$\partial p/\partial t + \mathbf{v}\cdot\nabla p_0 - c^2(\partial\varrho/\partial t + \mathbf{v}\cdot\nabla\varrho_0) = 0 \,; \tag{1c}$$

g is the gravity acceleration, c the sound speed and the subscripted quantities are the equilibrium ones.

The horizontal symmetry allows us, without loss of generality, to assume the wave vectors in a vertical plane (x, z), thus to ignore the y-coordinate. Fourier transforming in time and horizontal coordinate x, the system (1) becomes

$$i\omega\hat{\varrho} + \varrho_0(-ik\hat{v}_x + \partial\hat{v}_z/\partial z) + \hat{v}_z\,\partial\varrho_0/\partial z = 0 \,, \tag{2a}$$

$$i\omega\varrho_0\hat{v}_x - ik\hat{p} = 0 \,, \tag{2b}$$

$$i\omega\varrho_0\hat{v}_z + \partial\hat{p}/\partial z - g\hat{\varrho} = 0 \,, \tag{2c}$$

$$i\omega\hat{p} + \hat{v}_z\,\partial p_0/\partial z - c^2(i\omega\hat{\varrho} + \hat{v}_z\,\partial\varrho_0/\partial z) = 0 \,, \tag{2d}$$

where $\hat{v}_x$, $\hat{v}_z$ are the horizontal and vertical components of the fluid velocity, respectively, and $\hat{q}(z, k, \omega)$ indicates the Fourier transform of the function $q(z, x, t)$ defined as

$$\hat{q}(z, k, \omega) = \int_{-\infty}^{\infty}\int q(z, x, t)\exp[-i(kx - \omega t)]\,\mathrm{d}x\,\mathrm{d}t \,. \tag{3}$$

Introducing the divergence of the fluid velocity

$$\hat{\chi}(z, k, \omega) = \nabla \cdot \hat{\mathbf{v}}(z, k, \omega) = -ik\hat{v}_x(z, k, \omega) + \partial \hat{v}_z(z, k, \omega)/\partial z \tag{4}$$

and dropping the superscript $\hat{}$ for simplicity, we can obtain a single second-order ordinary differential equation for χ:

$$c^2 \frac{\mathrm{d}^2 \chi(z, k, \omega)}{\mathrm{d}z^2} + \left(\frac{\mathrm{d}c^2}{\mathrm{d}z} - \gamma g \right) \frac{\mathrm{d}\chi(z, k, \omega)}{\mathrm{d}z} + \left(\omega^2 + \left(\frac{k}{\omega} \right)^2 Q \right) \chi(z, k, \omega) = 0 , \tag{5}$$

with γ the ratio of specific heats and

$$Q = -\omega^2 c^2 + (\gamma - 1) g^2 + g \, \mathrm{d}c^2/\mathrm{d}z . \tag{6}$$

Once χ is known, the other perturbed fluid quantities can be derived from the relations

$$v_z(z, k, \omega) = \frac{(\omega^2 c^2 \mathrm{d}\chi(z, k, \omega)/\mathrm{d}z + g(-\gamma\omega^2 + k^2 c^2) \chi(z, k, \omega))}{(g^2 k^2 - \omega^4)} , \tag{7}$$

$$p(z, k, \omega) = i(\varrho_0/\omega)(c^2 \chi(z, k, \omega) - g v_z(z, k, \omega)) , \tag{8}$$

while $v_x(z, k, \omega)$ and $\varrho(z, k, \omega)$ are obtained straightforwardly from eqs. (2*b*) and (2*c*), respectively. Note, however, that eq. (7) is singular for (ω, k) values taken along the curve $g^2 k^2 - \omega^4 = 0$. As we will see later, this fact rules out some solutions of eq. (5) as non-physical.

It is now useful to define a new independent variable (stretched variable) via the local scale height $c^2(z)/\gamma g$:

$$u = \gamma g \int_{z_0}^{z} \frac{\mathrm{d}z'}{c^2(z')} , \tag{9}$$

with z_0 a reference point and furthermore a new dependent variable,

$$\psi = \chi \exp[-u] . \tag{10}$$

Then eq. (5) is transformed into

$$\frac{\mathrm{d}^2 \psi(u, k, \omega)}{\mathrm{d}u^2} - q^2(u, k, \omega) \, \psi(u, k, \omega) = 0 , \tag{11}$$

with

$$q^2(u, k, \omega) = \left(\frac{c^2(u)}{\gamma^2 g^2} \right) \left(-\omega^2 + \left(\frac{\gamma g}{2c(u)} \right)^2 + \right.$$

$$\left. + k^2 c^2(u) \left(1 - \frac{(\gamma - 1) g^2}{\omega^2 c^2(u)} \left(1 + \frac{\gamma}{\gamma - 1} \frac{\mathrm{d}}{\mathrm{d}u} \ln (c^2(u)) \right) \right) \right) . \tag{12}$$

Let us find out if and under which conditions horizontally guided modes do exist. We first recall that guided modes correspond to solutions of eq. (11) which tend to zero as $u \to \pm \infty$.

Physically this condition implies that the total kinetic energy per unit column associated with the wave remains finite.

Equation (11), with the above boundary conditions, is a particular case of the general eigenvalue equation

$$L\psi = E\psi \,, \tag{13}$$

where L is the Schrödinger operator $(-\mathrm{d}^2/\mathrm{d}u^2 + V(u))$, and $V(u)$ the potential function. In our case the potential function is $q^2(u, k, \omega)$ and we want to find, varying k, ω on the real axis, the bound states which correspond to zero energy.

In the appendix we will discuss sufficient conditions for the existence of bound states of eq. (11). We will actually prove the following:

Theorem: Let $c(u)$ be a continuous, monotonically increasing function of the variable u. Let also

$$c^2(u) - c_1^2 \simeq |u|^{-\alpha_1}, \qquad u \to -\infty \,, \tag{14a}$$

$$c^2(u) - c_2^2 \simeq -|u|^{-\alpha_2}, \qquad u \to +\infty \,, \tag{14b}$$

where $\alpha_1 > 1$, $\alpha_2 > 1$ are real constants, and $c_1 < c_2$ are the asymptotic values of the sound speed.

Then there exist at least two pairs of real, positive values $(k_i^2, \omega_i^2) i = 1, 2$ such that eq. (13) has a bound state at zero energy whenever the gradient of the sound speed profile has an upper bound which satisfies the relation

$$\max_{u \in \mathcal{R}} \left(\frac{\mathrm{d}c^2}{\mathrm{d}u} \right) \leqslant (\gamma - 2(\gamma - 1)^{1/2}) \frac{c_1^2 c_2^2}{c_1^2 + c_2^2} \,. \tag{15}$$

The above condition is only sufficient and is, moreover, too restrictive, as we will see in the next section. What is important, however, is that waves can be guided by a general class of smooth, monotonic sound speed profiles, and this result is not restricted to a particular, analytical choice of $c(u)$. Furthermore, the guided modes are not surface waves such as those studied by Thome, 1968, in the presence of a discontinuity in the profile, but, on the contrary they exist for very shallow gradients of the fluid temperature.

Moreover, although the proof is given only for the class of profiles satisfying the conditions of the previous theorem, a second important result is that two branches of solutions of eq. (11) are always present together: they correspond, whenever they are physically meaningful, to the acoustic and the acoustic-gravity branch.

3. – The hyperbolic tangent model

In order to better clarify the physical results illustrated above, let us consider a particular atmospheric model, which has the advantage that the eigenvalue equation (11) has analytic solutions. Moreover, it gives a realistic fit to the average atmospheric sound speed profile but for the two local minima at the mesopause and tropopause, as shown in fig. 1 (the dashed curve is the average sound speed profile, as reported, *e.g.*, by Francis, 1973). Note that the absence of the above-mentioned local minima is precisely what we want in order to discriminate between different possible driving

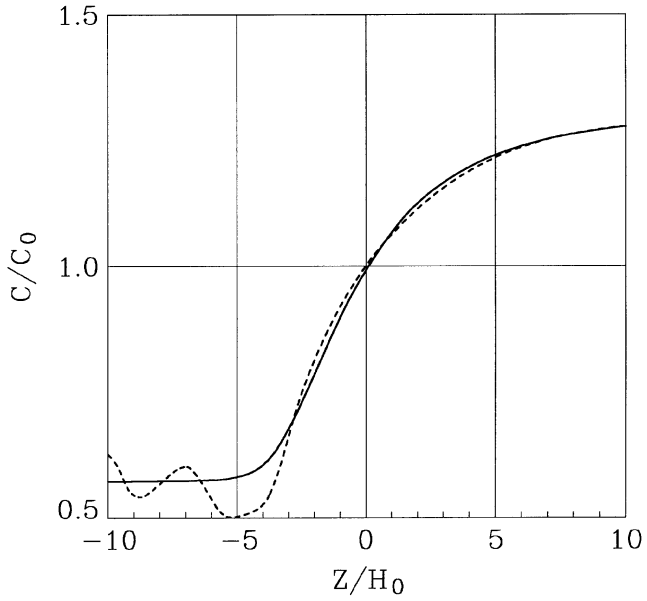

Fig. 1. – Normalized Earth's sound speed profile c/c_0, as a function of normalized height z/H_0. Dashed curve: average experimental profile, continuous curve: analytic hyperbolic tangent profile with $c_0 = 533\ \mathrm{m/s}$, $\delta = 0.673$, $d = 0.2$.

mechanisms. We, therefore, assume the following profile (hyperbolic tangent model):

$$c^2(u) = c_0^2(1 + \delta \tanh(\mathrm{d}u)) , \tag{16}$$

where

$$c_0^2 = \frac{c_1^2 + c_2^2}{2} , \tag{17a}$$

$$\delta = \frac{c_2^2 - c_1^2}{c_1^2 + c_2^2} , \tag{17b}$$

$$d = \frac{(\mathrm{d}c^2/\mathrm{d}u)_{\max}}{(c_2^2 - c_1^2)} . \tag{17c}$$

d is, therefore, a free parameter giving the slope of the sound speed profile.

As is discussed in Nalesso and Jacobson, 1993, by considering a new transformation:

$$s = \frac{1 + \tanh(\mathrm{d}u)}{2} , \tag{18a}$$

$$\Phi(s) = s^{-\beta}(s-1)^{-\alpha}\Psi(u(s)) , \tag{18b}$$

we have that Φ satisfies the hypergeometric equation, and therefore we obtain

$$\Psi(s) = s^{\beta}(s-1)^{\alpha} F(a,\, b;\, 1+2\beta;\, s)\,, \tag{19}$$

with $F(a,\, b;\, 1+2\beta;\, s)$ representing the hypergeometric function (Abramowitz and Stegun, 1972) and

$$a(k,\, s) = \alpha + \beta + 1/2 + \eta\,, \tag{20a}$$

$$b(k,\, s) = \alpha + \beta + 1/2 - \eta\,, \tag{20b}$$

whereas

$$\alpha(k,\, \omega) = \frac{1}{2d}\left[1/4 - \omega^2\,\frac{c_2^2}{\gamma^2 g^2} + k^2\,\frac{c_2^4}{\gamma^2 g^2}\left(1 - \frac{(\gamma-1)\,g^2}{\omega^2 c_2^2}\right)\right]^{1/2}, \tag{21a}$$

$$\beta(k,\, \omega) = \frac{1}{2d}\left[1/4 - \omega^2\,\frac{c_1^2}{\gamma^2 g^2} + k^2\,\frac{c_1^4}{\gamma^2 g^2}\left(1 - \frac{(\gamma-1)\,g^2}{\omega^2 c_1^2}\right)\right]^{1/2}, \tag{21b}$$

$$\eta(k,\, \omega) = \left[1/4 + \frac{k^2}{4d^2}\left(\left(\frac{c_2^2 - c_1^2}{\gamma g}\right)^2 + \frac{2d}{\gamma\omega^2}\,(c_2^2 - c_1^2)\right)\right]^{1/2}. \tag{21c}$$

By imposing the boundary conditions $\psi \to 0$ as $u \to \pm\,\infty$, we obtain that there are solutions *if and only if* the function $b(k,\, \omega)$ is equal to zero or a negative integer. This condition gives the dispersion relation for guided waves, which reads

$$\begin{aligned} D(k,\, \omega) = n + \frac{1}{2d}\left[1/4 - \omega^2\,\frac{c_2^2}{\gamma^2 g^2} + k^2\,\frac{c_2^4}{\gamma^2 g^2}\left(1 - \frac{(\gamma-1)\,g^2}{\omega^2 c_2^2}\right)\right]^{1/2} + \\ + \frac{1}{2d}\left[1/4 - \omega^2\,\frac{c_1^2}{\gamma^2 g^2} + k^2\,\frac{c_1^4}{\gamma^2 g^2}\left(1 - \frac{(\gamma-1)\,g^2}{\omega^2 c_1^2}\right)\right]^{1/2} + \\ + 1/2 - \left[1/4 + \frac{k^2}{4d^2}\left(\left(\frac{c_2^2 - c_1^2}{\gamma g}\right)^2 + \frac{2d}{\gamma\omega^2}\,(c_2^2 - c_1^2)\right)\right]^{1/2} = 0\,, \end{aligned} \tag{22}$$

with n zero or a positive integer. The corresponding eigenfunctions become

$$\begin{aligned} \chi_n(u,\, k,\, \omega) = \exp\left[u/2\right] \sum_{m=0}^{n} \frac{(-1)^n\, n!\, \Gamma(a+m)\, \Gamma(1+2\beta)}{(n-m)!\, m!\, \Gamma(m+1+2\beta)\, \Gamma(a)} \cdot \\ \cdot \left(\frac{-1}{1+\exp\left[2du\right]}\right)^{\alpha} \left(\frac{1}{1+\exp\left[-2du\right]}\right)^{\beta+m}, \end{aligned} \tag{23}$$

where Γ is the gamma-function.

The other physical quantities are easily derived from (2), (7), (8). They read, in terms of χ_n and its derivative $\mathrm{d}\chi_n/\mathrm{d}u$,

$$v_{zn}(u,\, k,\, \omega) = \left(\frac{\omega^2}{g^2 k^2 - \omega^4}\right)\left(\gamma g\,\frac{\mathrm{d}\chi_n(u,\, k,\, \omega)}{\mathrm{d}u} - g\left(\gamma - \frac{k^2 c^2}{\omega^2}\right)\chi_n(u,\, k,\, \omega)\right), \tag{24a}$$

$$(24b)\qquad v_{xn}(u,k,\omega)=\left(\frac{-ik}{g^2k^2-\omega^4}\right)\left((\gamma g^2)\frac{\mathrm{d}\chi_n(u,k,\omega)}{\mathrm{d}u}-(\gamma g^2-\omega^2c^2)\chi_n(u,k,\omega)\right),$$

$$(24c)\qquad \frac{p_n(u,k,\omega)}{\varrho_0(u)}=\left(\frac{-i\omega}{g^2k^2-\omega^4}\right)\left((\gamma g^2)\frac{\mathrm{d}\chi_n(u,k,\omega)}{\mathrm{d}u}-(\gamma g^2-\omega^2c^2)\chi_n(u,k,\omega)\right),$$

$$(24d)\qquad \frac{\varrho_n(u,k,\omega)}{\varrho_0(u)}=\left(\frac{-i\omega}{g^2k^2-\omega^4}\right)\left(\frac{\gamma^2g^2}{c^4}(c^2+\mathrm{d}c^2/\mathrm{d}u)\frac{\mathrm{d}\chi_n(u,k,\omega)}{\mathrm{d}u}-\right.$$
$$\left.-\left(\frac{g^2k^2-\omega^4}{\omega^2}+\frac{\gamma g^2}{c^4}\left(\gamma-\frac{k^2c^2}{\omega^2}\right)(c^2+\mathrm{d}c^2/\mathrm{d}u)\right)\chi_n(u,k,\omega)\right).$$

Finally, the kinetic energy per unit column is

$$(25)\quad W_n=\frac{1}{2}\varrho_0(u)(v_{xn}^2+v_{zn}^2)=\frac{1}{2}\varrho_0\left(\frac{\gamma^2g^2}{g^2k^2-\omega^4}\right)\left(\left(\frac{\mathrm{d}\chi_n}{\mathrm{d}u}-\chi_n\right)^2-\left(\frac{kc^2}{\gamma g}\right)^2\chi_n^2\right),$$

while the total kinetic energy per unit column is just the integral of W_n, with u ranging from $-\infty$ to $+\infty$.

A close inspection of the dispersion relation (22) shows, indeed, the existence of two families (the acoustic and the acoustic-gravity) of guided modes, as predicted by the theory, and allows us to understand their characteristics.

It is useful to express the dispersion curves of these modes as a function of two dimensionless quantities, the normalized radian period (ω_{b0}/ω) with $\omega_{b0}=(\gamma-1)^{1/2}g/c_0$ the buoyancy frequency at c_0 and (v_p/c_0) the phase velocity $v_p=(\omega/k)$ normalized to c_0. In the plane $(\omega_{b0}/\omega,\ v_p/c_0)$ the curves of the acoustic family begin and end at the acoustic cut-off lines (curves A_1 and A_2 in fig. 2) for internal waves propagating in isothermal media corresponding to low c_1 and high c_2 sound speed; note that these curves do not depend on the form of the profile. The number of acoustic modes depends on the sound speed gradient, a measure of which is the parameter d, and decreases as the gradient increases.

However, the $n=0$ acoustic mode, *i.e.*, the high phase velocity solution of the dispersion relation (22) corresponding to $n=0$, is not a real guided wave. In fact, it is readily recognized that this particular solution corresponds to $(\omega,\ k)$ values belonging to the curve $g^2k^2-\omega^4=0$ or, more precisely, to the segment shown as a dashed line in fig. 2, which is a portion of the curve represented by the previous equation. This dispersion curve, although mathematically correct and corresponding to eigensolutions of eq. (11) satisfying the prescribed boundary conditions, is not a real guided sound wave, as already observed. This is easily understood by observing that all the physically relevant quantities given by eqs. (24) are singular along the previous curve. Therefore, the acoustic family begins with the $n=1$ mode and can exist only up to a maximum value of the gradient, which depends on the profile parameters.

The acoustic-gravity family exhibits a different behavior as a function of the parameter d. For $d<d_{cr}=(\gamma-1)/2\gamma$, which corresponds to rather shallow sound speed profiles, we found a finite number of modes (as for the acoustic family), which begin and end at the corresponding acoustic-gravity cut-off lines A_{g1} and A_{g2} (see figs. 2 and 3). Again, the number of modes increases as d decreases.

However, for higher temperature gradients, *i.e.* for $d>d_{cr}$, the number of modes becomes infinite. The fundamental $(n=0)$ acoustic-gravity mode still begins at the

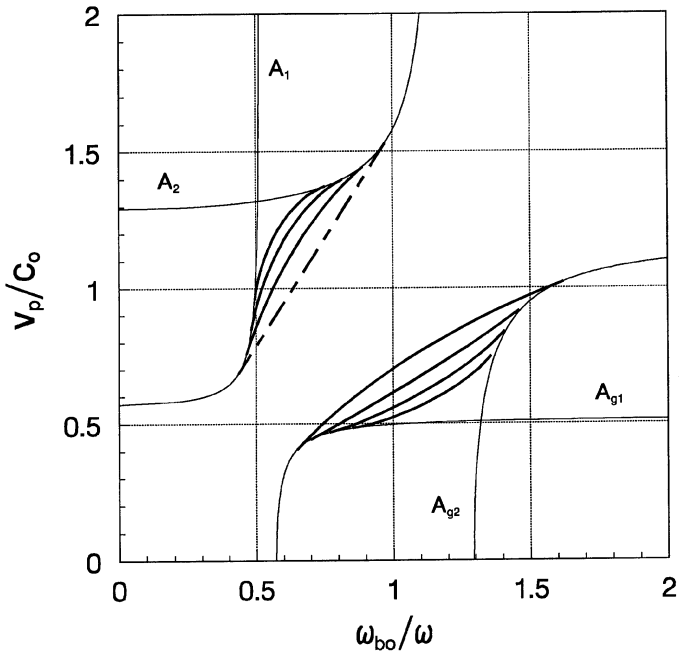

Fig. 2. – Dispersion curves (solid lines) for the hyperbolic tangent profile with $c_0 = 533\,\mathrm{m/s}$, $\delta = 0.673$, $d = 0.04$.

cut-off line A_{g2}, at very low frequency, but it ends with zero phase velocity at the point $\omega = \omega_d$:

$$\frac{\omega_{b0}}{\omega_d} = \left\{ \frac{2(c_1 c_2/c_0^2)^2 \delta(d/d_{cr})}{(\delta(d/d_{cr}) + 1)^2 - (c_1 c_2/c_0^2)^2} \right\}^{1/2}. \tag{26}$$

Note that ω_d is higher than the highest Brunt frequency in the entire system. To the same frequency (ω_{b0}/ω_d), still with zero phase velocity, tend also all the higher-order $(n > 0)$ modes, whose dispersion curves can begin, however, either at the upper cut-off line A_{g2}, or at the lower one A_{g1} (see fig. 4). In fig. 3 the dispersion curves for the sound speed profile which best fits the average atmospheric ones (shown as a continuous line in fig. 1) are presented. The characteristic parameters are: $\delta = 0.673$, $c_0 = c(z_0) = 533\,\mathrm{m/s}$, $z_0 = 160\,\mathrm{km}$, $d = 0.2$. Although the value of the parameter d is above the critical one, only a finite number $(n = 2)$ of acoustic-gravity modes can be appreciated because the accumulation point of all these modes lies too near to the high buoyancy frequency ω_{b1}.

Although the total kinetic energy per unit column is finite for every (k, ω) belonging to the dispersion curves, as is easy to verify since

$$W(u, k, \omega) \simeq \exp[-2d\alpha u] \to 0\,, \qquad \text{as } u \to \infty\,,$$

$$W(u, k, \omega) \simeq \exp[2d\beta u] \to 0\,, \qquad \text{as } u \to -\infty\,,$$

the dilatation χ_n as well as all the other physical quantities (24) may have a different

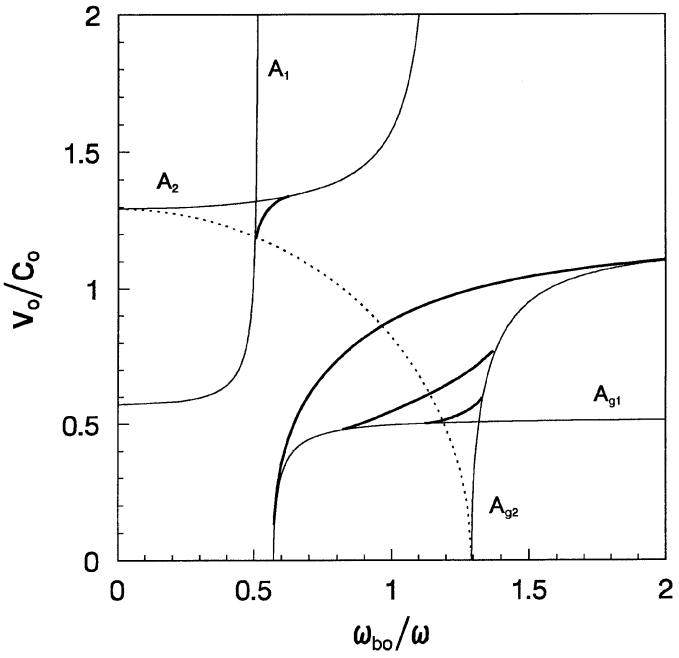

Fig. 3. – Dispersion curves (solid lines) for the hyperbolic tangent profile with $c_0 = 533\,\mathrm{m/s}$, $\delta = 0.673$, $d = 0.2$. The dotted line is the curve (arc of circle) $\alpha = 1/4d$.

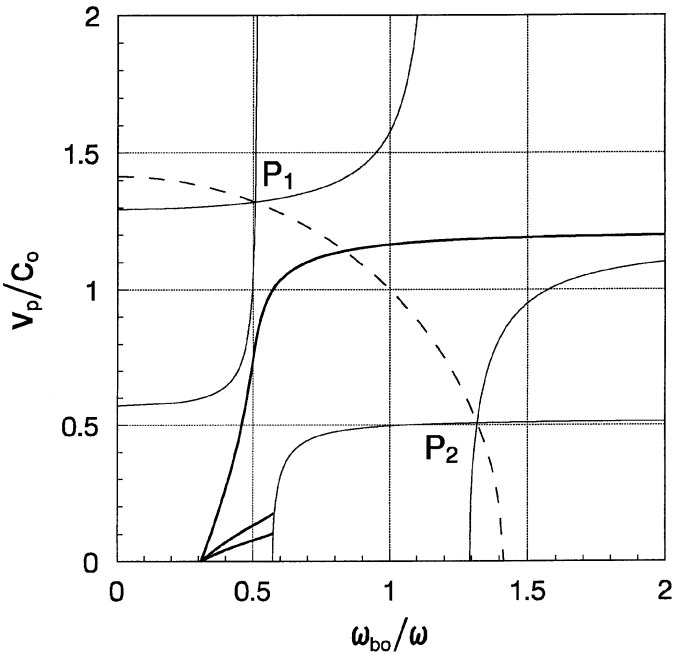

Fig. 4. – Dispersion curves (solid lines) for the hyperbolic tangent profile with $c_0 = 533\,\mathrm{m/s}$, $\delta = 0.673$, $d = 2.0$. The dashed line is the curve (arc of circle) $\Lambda(k, \omega) = 0$ (eq. (A.2)).

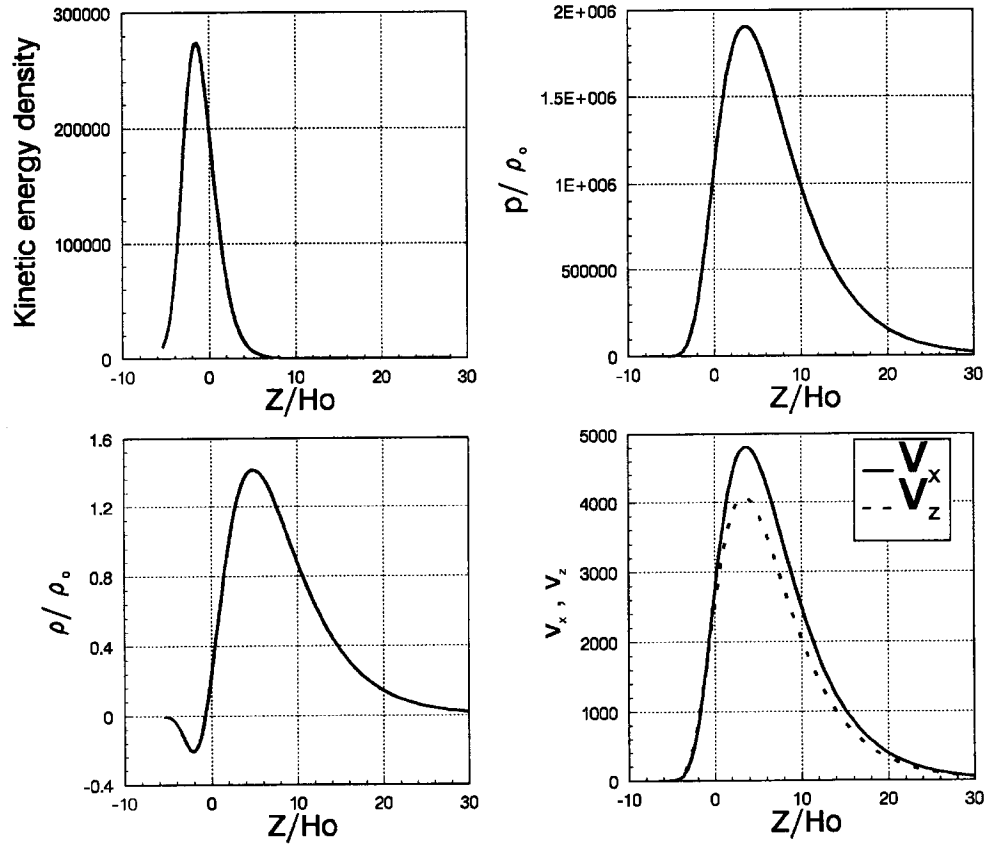

Fig. 5. – Kinetic energy density, pressure and density variations p/ϱ_0, ϱ/ϱ_0, horizontal and vertical components of the fluid velocity v_x, v_z as a function of z/H_0, for the $n=0$ acoustic-gravity mode with normalized radian frequency $\omega_{b0}/\omega = 0.8$ and the sound speed profile of fig. 1.

behavior for $u \to \infty$. In fact, if $2d\alpha < 1/2$, we observe that χ_n diverges to infinity with $u \to \infty$, while when $2d\alpha > 1/2$ the eigenfunctions tend to zero for $u \to \infty$. The region characterized by the first kind of behavior is shown in fig. 3; it lies on the right of the curve shown in the figure (dotted line) joining the points $(0, c_2/c_0)$ and $(c_2/c_0, 0)$. In the region on the left of the same curve we have, on the contrary, the second type of behavior. Let us point out, however, that the existence of unbounded eigenfunctions has only a mathematical relevance. Physically they cannot exist, because the inclusion of even an extremely small amount of viscosity or thermal conductivity will damp out these waves. An example of both types of waves is shown in figs. 5 and 6. In fig. 5 the kinetic energy density toghether with pressure and density variations, normalized to the equilibrium density ϱ_0, and the horizontal and vertical component of the fluid velocity of an acoustic-gravity wave $(n=0)$ are plotted as a function of the height, normalized to the scale height $H_0 = \gamma g/c_0^2$. Note that the vertical scales, although meaningful relative to each other, are nevertheless determined by the arbitrary normalization condition $\chi_{max} = 1$. They correspond to the sound speed profile shown in

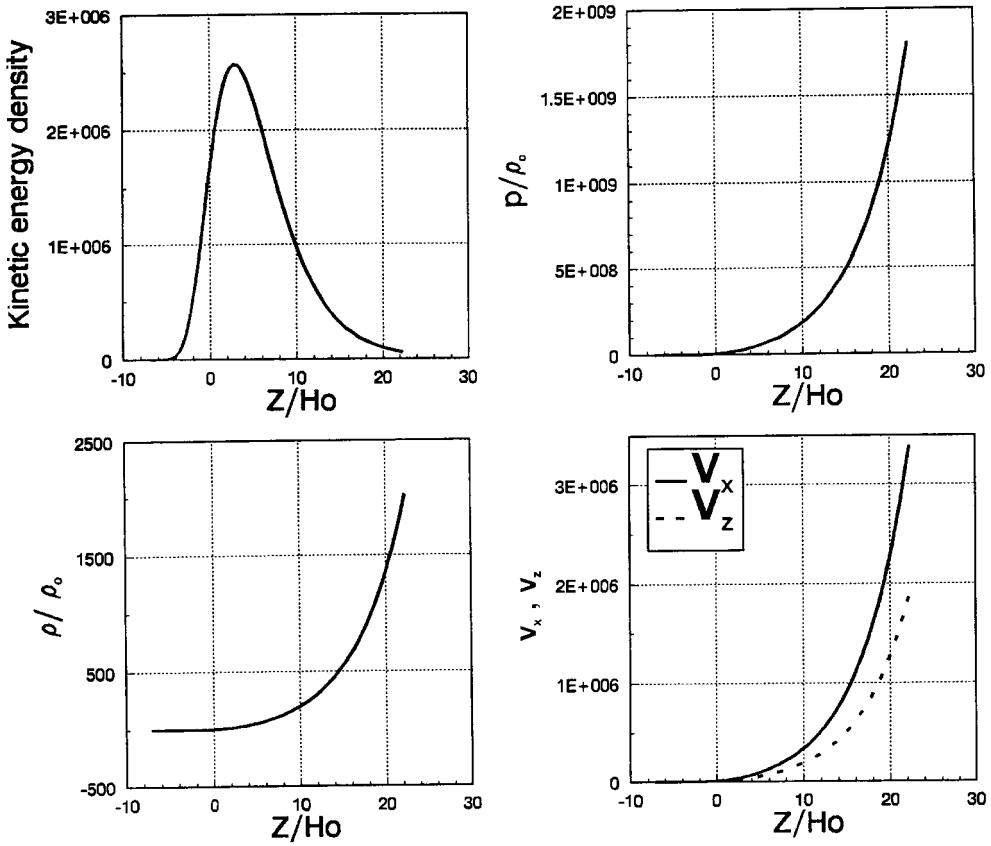

Fig. 6. – The same as fig. 5, but for the $n = 0$ acoustic-gravity mode with normalized radian frequency $\omega_{b0}/\omega = 1.3$.

fig. 1 (continuous line) and a normalized radian frequency $\omega_{b0}/\omega = 0.8$. The same quantities for a normalized radian frequency $\omega_{b0}/\omega = 1.3$ are plotted in fig. 6. It is of some interest to investigate how the number of modes and their dispersion relation evolve as the gradient steepness $d \to \infty$. We have already discussed the acoustic family and have pointed out that no acoustic modes can be guided when the temperature gradient becomes too high.

On the contrary, of the acoustic-gravity family, the fundamental ($n = 0$) mode survives, therefore the results of a step-like variation of the sound speed, namely the existence of a single guided surface mode, are recovered in this limit. Let us stress, however, that the diffuse profile case is much more general and shows a richer variety of guided waves.

4. – Inclusion of the Earth's surface: Lamb's modes

The model considered so far of an atmosphere extending to infinity both upward and downward is obviously not realistic. It has been introduced in order to study the

guiding properties of the thermocline in the simplest model, therefore avoiding the inclusion of other sources of guided modes.

However, a more physical model must include the Earth's surface, which will be considered here as a rigid plane surface, located, in the u coordinate system, at a fixed position u_0.

The boundary condition that must be imposed to any pressure wave at a rigid surface is simply that the orthogonal component of the fluid velocity is zero. This condition substitutes the previous one requiring that the solution of eq. (11) vanishes at $u \to -\infty$. However, to keep finite the total kinetic energy per unit column we still must have $\psi \to 0$ as $u \to \infty$ and this implies that the hypergeometric function appearing in (19) is regular at the point $s = 1$, corresponding to $u = \infty$. This can be accomplished assuming

$$\psi(u, k, \omega) = \left(\frac{1}{1+\exp[2du]}\right)^{\alpha}\left(\frac{1}{1+\exp[-2du]}\right)^{\beta} F\left(a, b; 1+2\alpha; \frac{1}{1+\exp[2du]}\right), \tag{27}$$

with α, β, a, b still given by (20), (21).

To satisfy the boundary condition at the rigid wall, we must set $v_z(u_0, k, \omega) = 0$. From (24a) the condition becomes

$$\left(\frac{\mathrm{d}\psi}{\mathrm{d}u}\right)_{u=u_0} = \left(\left(\frac{1}{2} - \frac{k^2 c^2}{\gamma \omega^2}\right)\psi\right)_{u=u_0} \tag{28}$$

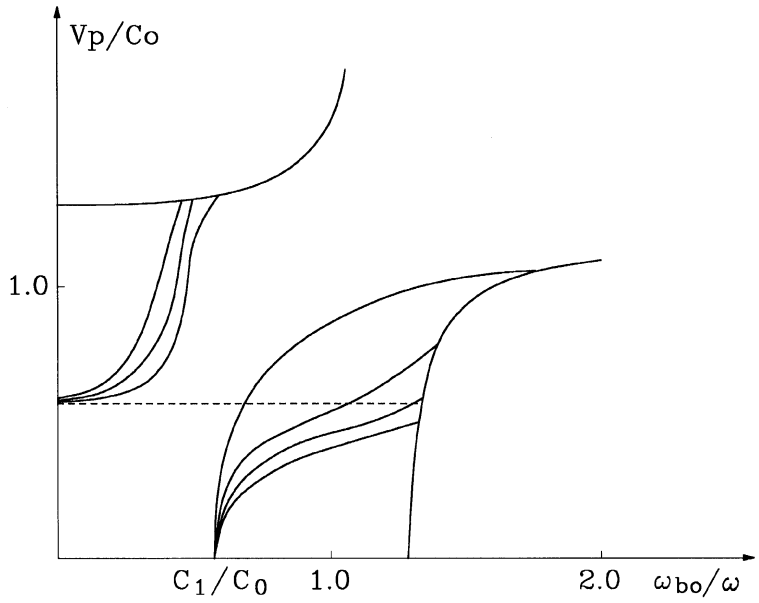

Fig. 7. – Dispersion curves for the hyperbolic tangent profile of fig. 1, with the Earth's surface placed at $u_0 = -25$ (corresponding to $z/H_0 = -10$). The dashed line represents Lamb's modes.

and using for ψ expression (27), we finally have the dispersion relation

$$(29)\quad \left[\left(-\frac{2d\alpha\exp[2du_0]}{(1+\exp[2du_0])}+\frac{2d\beta\exp[-2du_0]}{(1+\exp[-2du_0])}-\frac{1}{2}+\frac{k^2c^2}{\gamma\omega^2}\right)\cdot\right.$$

$$\cdot F\left(a,\,b;\,1+2a;\,\frac{1}{1+\exp[2du_0]}\right)-$$

$$\left.-\frac{2dab\exp[2du_0]}{(1+\exp[2du_0])^2(1+2\alpha)}F\left(a+1,\,b+1;\,2+2\alpha;\,\frac{1}{1+\exp[2du_0]}\right)\right]=0\,.$$

The analysis of the dispersion relation (29) shows that an infinite number of new higher-order modes, both in the acoustic and acoustic-gravity family, appears, regardless of the steepness of the thermocline. The dispersion curves of these modes, in the (ω_{b0}/ω), (v_p/c_0) plane, lie in the region where acoustic and acoustic-gravity free waves for an isothermal medium with sound speed equal to the highest value c_2 are forbidden.

Therefore, the acoustic-gravity modes extend to the previously forbidden region up to the cut-off line A_{g2}, while still accumulating, with zero phase velocity, at the frequency ω_d for $d > d_{cr}$. Moreover, for $d < d_{cr}$ the infinite number of higher-order modes which now exist, all converge to the lower buoyancy frequency ω_{b1}.

On the contrary, the acoustic modes do exist at very high frequency, actually also in the limit $\omega \to \infty$, with finite phase velocity.

This behavior is physically expectable, because the presence of the rigid wall allows the existence of waves propagating downwards and reflected by the wall. Kinetic

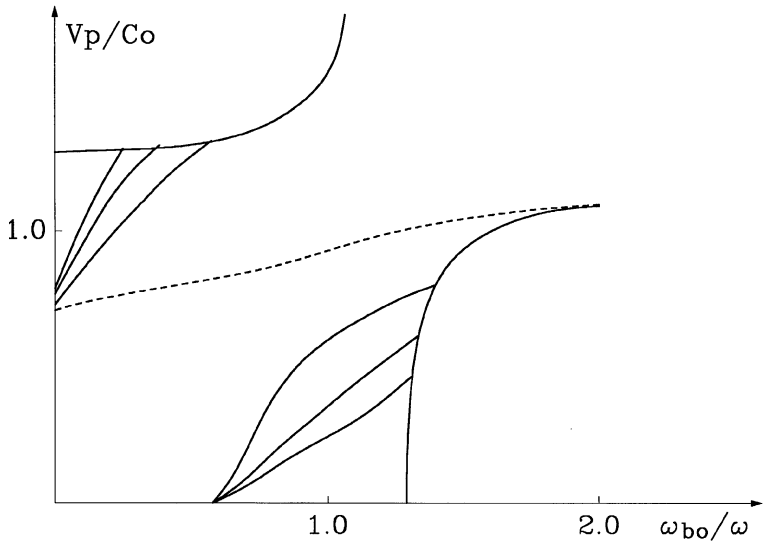

Fig. 8. – The same as fig. 7, but with the Earth's surface at $u_0 = -5$ $(z/H_0 = -3.5)$.

energy is not conveyed downwards to infinity, thus the constraint of a finite total energy per unit column can still be satisfied.

Let us note also that, if the rigid wall is not placed right in the thermocline (as it should be for a realistic model of the Earth's atmosphere), the modes driven by the thermocline, *i.e.* those existing without the rigid wall, are little affected by the presence of the wall. The main effect is in fact to extend the dispersion curves also to the previously forbidden regions down to the cut-off frequencies for the acoustic-gravity modes and to $\omega = \infty$ for the acoustic ones.

A second remarkable effect of the inclusion of the rigid wall is the appearance of a new type of wave, characterized by the kinetic energy peaked at the rigid wall. These are surface waves, and in fact they can be identified as Lamb's mode (Lamb, 1924; Francis, 1973). In the case of the Earth's surface far from the peak of the temperature gradient, ($u_0 = -25$, corresponding to the Earth's surface 160 km below the peak temperature gradient for the example shown in fig. 7), these waves are dispersionless with phase velocity very close to the local sound speed at the wall $c(u_0)$, and are well separated from the modes of the other two families (see dashed curve of fig. 7). However, when the rigid wall is moved toward the peak temperature gradient, Lamb's modes maintain their almost dispersionless character with phase velocity near $c(u_0)$ only at very high frequencies, while at lower frequencies they merge to the fundamental ($n = 0$) acoustic-gravity branch (see the dashed curve of fig. 8).

A comparison with the numerical results obtained by Francis shows indeed a good agreement, considering that the present model does not include dissipation (compare fig. 3 of Francis' 1973 article). The main, substantial difference is the absence of the "imperfectly ducted" modes, which, however, cannot exist in our model.

5. – The dissipative case

If dissipation, such as thermal conduction and viscosity, is taken into account, the wave motion is no longer adiabatic, because the effect of loss processes is to increase the total entropy with time. This means that the adiabatic equation (1*c*) must be replaced by the conservation of energy equation, and, to close the system, an equation of state has to be added.

In the dissipative case then, the linearized HD equations (2) must be substituted with (see Francis, 1973)

$$
\text{(30)} \qquad \begin{cases} i\omega\hat{\varrho} + \varrho_0(-ik\hat{v}_x + \partial\hat{v}_z/\partial z) + \hat{v}_z\,\partial\varrho_0/\partial z = 0\,, \\ i\omega\varrho_0\,\hat{v}_x - ik\hat{p} = \Phi_1, \\ i\omega\varrho_0\,\hat{v}_z + \partial\hat{p}/\partial z - g\hat{\varrho} = \Phi_2, \\ \dfrac{p_0}{(\gamma-1)\,T_0}(i\omega\hat{T} + (\partial T_0/\partial z)\,\hat{v}_z) + p_0(k\hat{v}_x + \partial\hat{v}_z/\partial z) = \Phi_3, \\ \gamma\hat{p} - c^2\hat{\varrho} - c^2(\varrho_0/T_0)\,\hat{T} = 0\,, \end{cases}
$$

where

$$(31)\qquad \begin{cases} \Phi_1 = -(4/3)\,\eta k^2 \hat{v}_x - (1/3)\,\eta k \partial \hat{v}_z/\partial z - k(\partial\eta/\partial z)\,\hat{v}_z + \dfrac{\partial}{\partial z}(\eta \partial \hat{v}_x/\partial z), \\ \Phi_2 = -\eta k^2 \hat{v}_z + (1/3)\,\eta k \partial \hat{v}_x/\partial z - (2/3)\,k(\partial\eta/\partial z)\,\hat{v}_x + (4/3)\dfrac{\partial}{\partial z}(\eta \partial \hat{v}_z/\partial z), \\ \Phi_3 = \lambda(\partial^2 \hat{T}/\partial z^2) - \lambda k^2 \hat{T} + (\partial\lambda/\partial z)(\partial \hat{T}/\partial z) \end{cases}$$

are the dissipative terms, $\eta(z)$ the viscosity and $\lambda(z)$ the thermal conductivity, and $\hat{}$ denotes, as usual, the Fourier transform.

In the dissipationless limit, the system (30) can be compactly written in matrix form

$$(32)\qquad D^0(\omega, z, \partial/\partial z)\,\psi(k, \omega, z) = kM\psi(k, \omega, z),$$

with D^0 a 5×5 matrix operator given by

$$(33)\qquad D^0 = \begin{vmatrix} 0, & -i\left(\dfrac{\partial}{\partial z}(\ln \varrho_0) + \dfrac{\partial}{\partial z}\right), & \omega, & 0, & 0 \\ \omega, & 0, & 0, & 0, & 0 \\ 0, & \omega, & ig, & -i\left(\dfrac{\partial}{\partial z}(\ln \varrho_0) + \dfrac{\partial}{\partial z}\right), & 0 \\ 0, & -i\left(\dfrac{1}{(\gamma-1)}\dfrac{\partial}{\partial z}(\ln T_0) + \dfrac{\partial}{\partial z}\right), & 0, & 0, & \dfrac{\omega}{(\gamma-1)\,T_0} \\ 0, & 0, & -c^2, & \gamma, & -c^2/T_0 \end{vmatrix};$$

M is a 5×5 constant matrix, and ψ a one-column vector of the Fourier transforms of the fluid variables

$$(34)\qquad M = \begin{vmatrix} 1, & 0, & 0, & 0, & 0 \\ 0, & 0, & 0, & 1, & 0 \\ 0, & 0, & 0, & 0, & 0 \\ 1, & 0, & 0, & 0, & 0 \\ 0, & 0, & 0, & 0, & 0 \end{vmatrix}, \qquad \psi = \begin{vmatrix} \hat{v}_x \\ \hat{v}_z \\ \hat{\varrho}/\varrho_0 \\ \hat{p}/\varrho_0 \\ \hat{T} \end{vmatrix}.$$

This can be looked at as an eigenvalue problem, whose eigenvalues k are, for each ω, the solutions of the dispersion equation (22), and the corresponding eigenvectors are given by (24), with the temperature $\hat{T}$ obtained from the last equation of system (30).

Coming back to the dissipative case and defining the dissipation matrix operator V through the relation

$$(35)\qquad V\psi = \Omega,$$

with Ω the one-column vector of components

$$\begin{cases} \Omega_1 = 0 , \\ \Omega_2 = (i/\varrho_0)\, \Phi_1 , \\ \Omega_3 = (i/\varrho_0)\, \Phi_2 , \\ \Omega_4 = (i/p_0)\, \Phi_3 , \\ \Omega_5 = 0 , \end{cases} \tag{36}$$

we arrive at the equation

$$(\boldsymbol{D}^0 + \boldsymbol{V})\, \psi = k \boldsymbol{M} \psi . \tag{37}$$

An approximate solution of this problem can be obtained in the frame of the perturbation theory, if the dissipation term $\boldsymbol{V}\psi$ can be considered as a small perturbation with respect to the dissipationless solution. The limits of this approach are obviously those intrinsic to the perturbative technique (Courant and Hilbert, 1953).

However, perturbation theory cannot be applied straightforwardly to this problem, because the zeroth-order operator $\boldsymbol{D}^0$ is not Hermitian and, as a consequence, the unperturbed eigenvectors are not orthogonal. In spite of this complication, after the coordinate transformation (9), we have worked out the first-order correction k_n^1 to the propagation constant of the n-th mode.

For any given ω, when N non-orthogonal eigenmodes are present, the first-order correction reads

$$k_n^{(1)} = - \sum_{j=1}^{N} a_{n,j}^{-1} V_{j,n} , \tag{38}$$

where $a_{i,j}^{-1}$ are the elements of the inverse of the matrix defined as

$$a_{i,j} = (k_j^{(0)} - k_n^{(0)})\, M_{i,j} - \delta_{j,n} M_{i,n} \tag{39}$$

($\delta_{j,n}$ is the Kronecker symbol) and

$$M_{i,j} = \int_{-\infty}^{+\infty} \exp[-u]\, \psi_i^*(u)\, \boldsymbol{M}\psi_j(u)\, \mathrm{d}u , \tag{40}$$

$$V_{i,j} = \int_{-\infty}^{+\infty} \exp[-u]\, \psi_i^*(u)\, \boldsymbol{V}\psi_j(u)\, \mathrm{d}u , \tag{41}$$

with $\boldsymbol{M}$ and $\boldsymbol{V}$ defined by eqs. (34), (35). These matrix elements represent inner products in the linear space of the solutions of the system (30).

The first-order correction $k_n^{(1)}$ obtained from eq. (38) is a complex quantity, because of the dissipative nature of the considered atmospheric model. Its real part gives the correction to the horizontal propagation constant k_n, while the imaginary part represents the (first order) attenuation factor.

An example is shown in fig. 9, for the equilibrium configuration of fig. 1. In the figure the real part (dashed line, left scale) and the imaginary part (continuous line, right scale) of the first-order correction $k^{(1)}$ to the fundamental ($n = 0$) acoustic-gravity mode, normalized to the zeroth-order wave number k_0 is plotted.

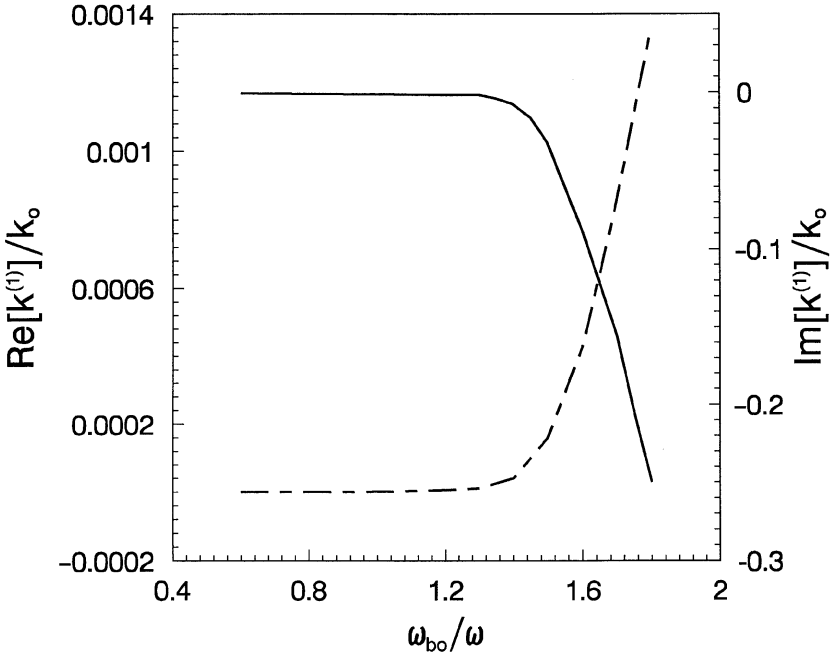

Fig. 9. – Real (dashed line, left scale) and imaginary (continuous line, right scale) part of the first-order correction to the $n = 0$ acoustic-gravity mode, normalized to the zeroth-order wave number k_0 for the hyperbolic tangent profile of fig. 1 with dissipation.

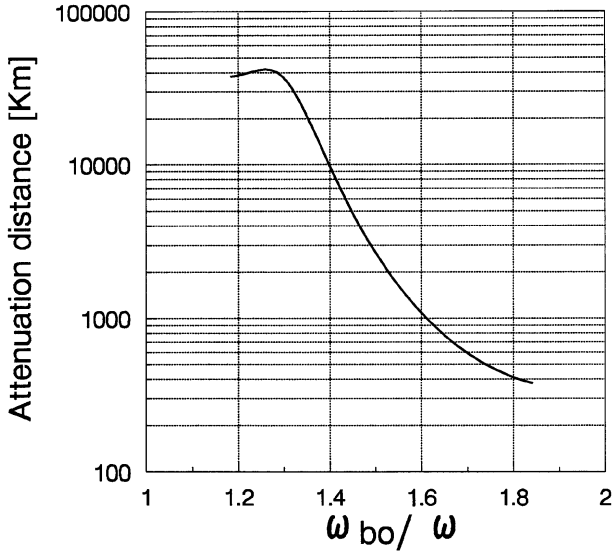

Fig. 10. – Attenuation distance *vs.* normalized radian period for the $n = 0$ acoustic-gravity modes with the same parameters as fig. 9.

Viscosity and thermal conductivity has been assumed of the form

$$\eta = 3.43 \cdot 10^{-7} T^{0.69} \quad (\mathrm{kg\,m^{-1}\,s^{-1}}), \tag{42}$$

$$\lambda = 38.2 \cdot 10^{-5} T^{0.69} \quad (\mathrm{kg\,m\,s^{-3}\,K^{-1}}) \tag{43}$$

(see Banks and Kockarts, 1973).

In the following fig. 10 the attenuation distance $(1/|\mathrm{Im}\{k^{(1)}\}|)$ is plotted as a function of (ω_{b0}/ω). It is clearly seen that long-period waves are strongly damped, as was anticipated. Waves whose amplitude becomes unbounded with increasing altitude are just a pathology of the non-dissipative mathematical model! Only medium–short-period waves, localized in the region where the thermocline gradient is appreciable, can propagate to distances comparable to the Earth's circumference.

Similar results are obtained also for the other guided modes.

6. – Conclusions

In this paper we have proved that there exists a class of horizontally ducted acoustic and acoustic-gravity waves, in a stratified, non-dissipative, windless atmosphere, which can be supported by the temperature gradient. Sufficient conditions have been derived which extend to a large class of monotonically increasing with height temperature profiles the guiding properties previously found for a particular model. Furthermore, the contemporary presence of two families of guided waves, namely the acoustic and the acoustic-gravity family, has also been demonstrated.

The spectrum of the guided modes, as a function of the profile parameters, has been explored by considering the above-mentioned temperature profile, which can be expressed in a closed analytical form (the hyperbolic tangent model). The results show an extraordinary richness of modes which can propagate, and these can account for practically all the experimental observation and the previous numerical results (Francis, 1973; Wang and Tuan, 1988). We have, then, included in the model the Earth's surface. It turned out to be essential in supporting Lamb's modes, *i.e.* almost dispersionless surface waves, localized near the rigid surface and an infinity of higher-order acoustic modes of very high frequency. On the contrary, the Earth's surface is not necessary, although it surely plays a role, for the existence of the acoustic-gravity family of guided modes.

A comparison of the results of our hyperbolic tangent model (including Earth's surface) with those published by Francis (1973, 1975) shows a very good agreement as long as the "fully ducted" modes are considered (imperfectly ducted modes cannot be accounted for in a dissipationless model).

These results allow us to conclude that the local mesopause and tropopause minima (not included in our model) have only local effects, *i.e.* they may change a little the dispersion curve only for modes localized near these minima. Therefore, the usual interpretation of experimental and numerical results, for medium–short-period gravity waves, relying on the presence of both a local minimum in the sound speed profile and a rigid surface (see, for instance, Wang and Tuan, 1988) is not unique. These waves, in fact, can exist even in the absence of both rigid surface and local minimum, and can be supported just by an appropriate thermocline.

Finally, we have included dissipation in the model. A perturbation technique has been used to derive first-order corrections to the propagation vector. In spite of the limits of the technique, and of the simplified treatment of the dissipative terms, the attenuation distance of the gravity modes is in reasonable agreement with the more sophisticated results of Francis' model.

As a general conclusion, our model has shown that dissipation is very effective in damping out those modes which, ideally, could grow, unbounded, at a very high altitude.

APPENDIX

We give now the proof of the

Theorem: Let $c(u)$ be

I1) a continuous, monotonically increasing function of the variable u.

I2) Let also:

$$c^2(u) - c_1^2 \simeq |u|^{-\alpha_1}, \qquad u \to -\infty ,$$
$$c^2(u) - c_2^2 \simeq -|u|^{-\alpha_2}, \qquad u \to +\infty ,$$

where $\alpha_1 > 1$, $\alpha_2 > 1$ are real constants, and $c_1 < c_2$ are the asymptotic values of the sound speed.

Then, there exist at least two pairs of real, positive values (k_i^2, ω_i^2) $i = 1, 2$ such that eq. (13),

$$L\psi(u) = E\psi(u) ,$$

has a bound state at zero energy whenever the gradient of the sound speed profile has an upper bound which satisfies the relation

$$\max_{u \in \mathscr{R}} \left(\frac{\mathrm{d}c^2}{\mathrm{d}u} \right) \leqslant (\gamma - 2(\gamma - 1)^{1/2}) \frac{c_1^2 c_2^2}{c_1^2 + c_2^2} . \tag{A.1}$$

Proof: It is easy to verify that, if $c(u)$ satisfies I1, and ω, k are taken on the curve l of equation

$$\Lambda(k, \omega) = \left(\frac{1}{c_0} \right)^2 \left(\frac{\omega}{k} \right)^2 + \left(\frac{\omega_{b0}}{\omega} \right)^2 - 2 = 0 , \tag{A.2}$$

i.e. along the arc of circle of radius $\sqrt{2}$ in the first quadrant of the (v_p/c_0), (ω_{b0}/ω) plane, then

$$q^2(-\infty) = q^2(\infty) = q_\infty^2 = \left(1/4 - k^2 \left(\frac{c_2^2 c_1^2}{\gamma^2 g^2} \right) \right), \tag{A.3}$$

and q_∞^2 is a continuous function of k^2, equal to zero for $k^2 = (\gamma g/2c_1c_2)^2$ (points P_1 and P_2 of fig. 4), and positive along the arc P_1P_2 (dashed line in fig. 4).

Define the new potential function:

$$V(u) = q^2(u) - q_\infty^2, \tag{A.4}$$

with $(\omega, k) \in l$.

Then, whenever hypothesis I2) is satisfied, $V(u) \to 0$ as $|u| \to \infty$, $V(u) \in L^2(R)$ and is an everywhere non-positive, not identically zero function of $u \in R$.

In these hypotheses, the Schrödinger operator $L = (-\mathrm{d}^2/\mathrm{d}u^2 + V(u))$ always has at least a bound state corresponding to a negative eigenvalue $\lambda < 0$ (see Reed and Simon, 1978; Rose and Weinstein, 1988). Moreover, $\lambda(k^2)$ is a continuous function of $k^2 \in l$ and satisfies

$$V_{\min}(k^2) < \lambda(k^2) = E(k^2) - q_\infty^2 < 0,$$

with $V_{\min}$ the minimum value of $V(u)$ for $u \in R$, $E(k^2)$ a continuous function of k^2 and also

$$q_{\min}^2(k^2) < E(k^2) < q_\infty^2,$$

with $q_{\min}^2$ obviously the minimum of $q^2(u)$, $u \in R$.

Because along the arc P_1P_2 it is $q_\infty^2 \geqslant 0$, the equality holding at the extrema, to prove that there exists a $k_0^2 \in P_1P_2$, such that $E(k_0^2) = 0$, it is *sufficient* to show that $q_{\min}^2(k^2) = 0$ at some point $P_0 \in P_1P_2$. It will be, in fact, $E(P_1) < 0$ and $E(P_0) > 0$, therefore, because of the continuity of the function E, there exists a point P such that $E(P) = 0$.

Note that the existence of such point ensures that at least two values k_{0i}^2 $(i = 1, 2)$ can always be found such that $E(k_{0i}^2) = 0$, and therefore the existence of two families of guided waves is also proved.

To prove the second part of the theorem, we need to find the minimum of the function $q^2(u, k, \omega)$, subject to the restriction $\Lambda(k, \omega) = 0$, with Λ given by eq. (A.2). This problem is solved with Lagrange's method of multipliers, which states that the desired minimum is the minimum of the function

$$\Psi(u, k, \omega) = q^2(u, k, \omega) + \varepsilon\Lambda(k, \omega), \tag{A.5}$$

with ε the Lagrange multiplier.

This problem has simple solutions for sound speed profiles such that the maximum of the gradient of $c^2(u)$ is attained at the point where $c^2 = (c_1^2 + c_2^2)/2 = c_0^2$. In this case

$$q_{\min}^2 = 1/4 - \frac{(\gamma - 1)\, c^2(2c_0^2 - c^2)}{4\gamma^2 c_0^4} \left\{ 1 + \left(1 + \frac{2\gamma c_0^2 (\mathrm{d}c^2/\mathrm{d}u)_{c = c_0}}{(\gamma - 1)\, c^2(2c_0^2 - c^2)} \right)^{1/2} \right\}^2. \tag{A.6}$$

A sufficient condition to have $q_{\min}^2 = 0$ on P_1P_2 is then given by condition (A.1) as it is easy to show.

Le us point out, however, that this condition is only sufficient. It shows that even sound speed profiles with very small gradients are able to guide acoustic and acoustic-gravity waves. In the other limit of very high gradient, even if a mathematical proof for general profiles has not been worked out, we know, at least for certain analytic profiles, that these waves are also guided.

REFERENCES

ABRAMOWITZ M. and STEGUN I. A., *Handbook of Mathematical Functions* (Dover, New York) 1972.

BANKS P. M. and KOCKARTS G., *Aeronomy* (Academic Press, New York) 1973.

COURANT R. and HILBERT D., *Methods of Mathematical Physics* (Interscience Publishers, New York) 1953.

FRANCIS S. H., *Acoustic-gravity modes and large-scale travelling ionospheric disturbances of a realistic, dissipative atmosphere*, *J. Geophys. Res.*, **78** (1973) 2278-2301.

FRANCIS S. H., *Global propagation of atmospheric gravity waves: A review*, *J. Atmos. Terr. Phys.*, **37** (1975) 1011-1054.

LAMB H., *Hydrodynamics* (Cambridge University Press, Cambridge) 1924.

NALESSO G. F. and JACOBSON A. R., *On a mechanism for ducting of acoustic and short-period acoustic-gravity waves by the upper atmospheric thermocline*, *Ann. Geophys.*, **11** (1993) 372-376.

PEKERIS C. L., *The propagation of a pulse in the atmosphere. Part II*, *Phys. Rev.*, **73** (1948) 145-154.

REED M. and SIMON B., *Methods of Modern Mathematical Physics IV: Analysis of Operators* (Academic Press, New York) 1978.

ROSE H. A. and WEINSTEIN M. I., *On the bound states of the nonlinear Schrödinger equation with a linear potential*, *Physica D*, **30** (1988) 207-218.

THOME G., *Long-period waves generated in the polar ionosphere during the onset of magnetic storms*, *J. Geophys. Res.*, **73** (1968) 6319-6336.

WANG D. Y. and TUAN T. F., *Brunt-Doppler ducting of small-period gravity waves*, *J. Geophys. Res.*, **93** (1988) 9916-9926.

YEH K. and LIU C. H., *Acoustic-gravity waves in the upper atmosphere*, *Rev. Geophys. Space Sci.*, **12** (1974) 193-216.